

PHYSICAL REVIEW LETTERS

VOLUME 43

24 DECEMBER 1979

NUMBER 26

Measurement of $\bar{p}p$ Backward Elastic-Scattering Cross Section from 406 and 922 MeV/c

M. Alston-Garnjost, R. P. Hamilton, R. W. Kenney, D. L. Pollard, and R. D. Tripp
Lawrence Berkeley Laboratory, University of California, Berkeley, California 94720

and

H. Nicholson

Mount Holyoke College, South Hadley, Massachusetts 01075

and

D. M. Lazarus

Brookhaven National Laboratory, Upton, New York 11973

(Received 7 August 1979)

The cross section for 180° elastic scattering of antiprotons by protons between 406 and 922 MeV/c has been measured. A single-arm spectrometer detected recoil protons corresponding to events with $\langle \cos\theta_{\text{c.m.}} \rangle = -0.994$. The regions of the reported resonances at 1936 and 2020 MeV were scanned in 10-MeV/c steps with a typical statistical error of $\approx 7\%$ and an rms mass resolution of ± 3 MeV. No narrow enhancements ($\Gamma < 10$ MeV) were observed.

Since 1966, when structures in the $\pi^-p \rightarrow pX^-$ missing-mass spectrum were reported at 1929, 2195, and 2382 MeV by the CERN Missing Mass Spectrometer Group,¹ many claims for narrow boson resonances near these masses have appeared in the literature. In addition to the S , T , and U peaks, a narrow resonance has recently been observed in the $\bar{p}p$ system at 2020 MeV along with the $T(2204)$ in the reaction $\pi^-p \rightarrow (\pi^-p_f)\bar{p}p$, where the (π^-p_f) form a fast Δ or N^* and the $\bar{p}p$ system is slow in the laboratory.² Several formation experiments indicating structure in $\bar{p}p$ and $\bar{p}d$ total cross sections³⁻⁵ and $\bar{p}p$ elastic^{4,6} and annihilation^{6,7} cross sections have given some credence to at least the S meson at 1936 MeV.⁸ However, evidence to the contrary has also been published⁹⁻¹³ and our measurement of the charge-exchange cross section $\sigma(\bar{p}p \rightarrow \bar{n}n)$ has shown no evi-

dence for the resonance.¹⁴

In this Letter we report the results of a counter experiment performed in the Brookhaven alternating-gradient synchrotron low-energy separated beam, in which the backward elastic $\bar{p}p$ differential cross section ($\langle \cos\theta_{\text{c.m.}} \rangle = -0.994$) was measured at 30 momenta between 406 and 922 MeV/c. Backward scattering is favorable for the observation of resonances since the differential cross section for $\bar{p}p$ scattering is known to be small in the backward direction (typically 100 times smaller than the forward diffraction peak in our momentum region), while a purely resonant amplitude, if it exists, must always be present at $\cos\theta = \pm 1$. The resonant differential cross section at $\cos\theta = \pm 1$ is greater than or equal to $\sigma_{\text{el}}^{\text{res}}/4\pi$ for all values of J^{PC} , with the inequality generally becoming stronger as the spin J of the resonance in-

creases.^{15,16} With use of the measured value for the contribution of the S meson to the elastic cross section of 7 ± 1.4 mb,⁴ we obtain an expected resonant contribution to the backward differential cross section of at least 0.5 mb/sr which is comparable to the observed nonresonant background. However, interference between the resonance and background may be constructive or destructive depending on whether J is odd or even, so that larger or smaller effects may be anticipated. For example, a pathological case could lead accidentally to a complete suppression of resonant structure if the nonresonant amplitude were half as large and of opposite phase to the resonant amplitude. Previously published data on $\bar{p}p$ backward elastic scattering,^{17,18} shown in Fig. 3(a), are of low statistical accuracy and agreement between the two experiments is very poor.

The apparatus, originally designed to measure K^-p backward elastic scattering,¹⁹ is shown in Fig. 1. The incident beam geometry was defined by thin scintillators M and S . The mass-slit counter (MS) located 5 m upstream of M facilitated time-of-flight measurements. A threshold Cherenkov counter (C) rejected mesons. Additional suppression of beam mesons was obtained by pulse-height discrimination on counters S and M . A lead collimator with an aperture for beam passage was placed between counters C and M . This collimator reduced the number of backward-going π^+ 's that could have entered C and vetoed the event, the π^+ 's having been produced in the annihilations of stopped \bar{p} 's from backward elastic scatters. Immediately downstream of the 20.96-cm-long liquid-hydrogen target ($\rho = 0.070$ g/cm³) was a bending magnet ($D4$) that swept away the unscattered beam and the unwanted charged particles at 0° . The recoil protons were then focused through the second bending magnet ($D5$) by the quadrupole doublet ($Q7$ and $Q8$) onto the hodoscope

(H) which had 45 vertical channels each 1.27 cm wide. The image of the target was centered on the hodoscope and was about 22 cm wide. The outer hodoscope channels were used to measure background. A timing counter (T) behind H was used to identify protons by measuring the time of flight over the 8.5-m flight path between M and T . The acceptance of the spectrometer (9.8 msr) was defined primarily by a thin counter (P) 25.4 cm high and 7.6 cm wide, placed 140.4 cm downstream of the target center. In addition, the acceptance was limited slightly by the apertures of the magnets.

An incident \bar{p} was identified electronically as $\varphi = M \cdot S \cdot \bar{C}$ and included time of flight of the \bar{p} from MS to M and pulse height in M and S . Misidentification of mesons in the beam was negligible at low momenta and rose to 1.7% at the highest momenta. A \bar{p} backward elastic trigger was $\varphi \cdot P \cdot \Sigma_i H_i$ placed in coincidence with a gate generated from the proton time of flight from M to T .

Kinematics and good time-of-flight separation resulted in excellent signal to background in the hodoscope distributions (Fig. 2). Empty-target rates, typically 15% of the target-full rates, were measured at each momentum and subtracted. After this subtraction, no statistically significant background was observed in the outer channels of the hodoscope.

In the region of the S meson, the experimental energy resolution was dominated by energy loss in the hydrogen target. In addition there was a contribution due to the beam-momentum spread which was calculated from beam optics and confirmed by \bar{p} -range measurements. At 505 MeV/ c the rms momentum resolution was ± 12 MeV/ c or ± 2 MeV in the c.m. system.

Multiplicative corrections to the measured cross sections are small. Ranges given below are for increasing incident momentum.

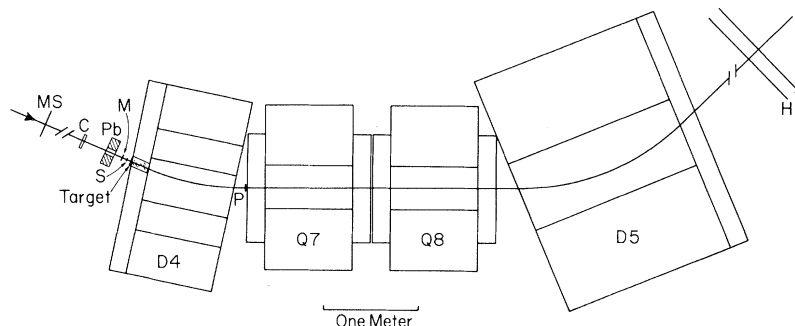


FIG. 1. The experimental apparatus.

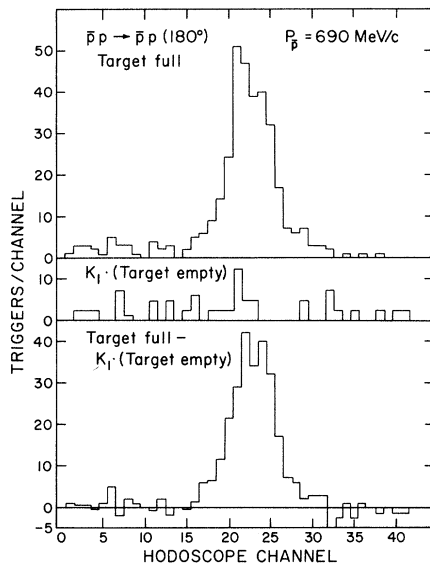


FIG. 2. Typical distributions on the hodoscope of target-full and normalized empty-target data, and the subtracted results. $K_1 = \varphi_F/\varphi_{MT}$, the ratio of incident beam fluxes with target full and empty.

(1) Correction for beam mesons that are misidentified as antiprotons. Since events produced by π^- are kinematically distinguishable from true events only the correction to the incident \bar{p} flux is significant. This measured correction varied from 1.0 to 1.017.

(2) Absorption of antiprotons in the liquid-hydrogen target was calculated from published data.²⁰ The correction exhibited a smooth variation from 1.086 to 1.051.

(3) Correction for spectrometer acceptance included recoil-proton absorption in the hydrogen target, P counter, and air path. This was determined by Monte Carlo calculation to vary smoothly from 1.270 to 1.045 (1.10 at 500 MeV/c).

(4) There were four momentum-independent corrections at the 1% level: (a) absorption of \bar{p} in the beam counter S_2 , (b) beam profile and target shape, determined by beam multiwire proportional counters and target x rays, respectively, (c) recoil protons absorbed in the acceptance defining counter P and air path between target and H hodoscope, and, (d) backward scattering events which were vetoed by pions arising from annihilation of the stopped antiprotons and emitted backward into the Cherenkov counter.

The corrected differential cross section for $\bar{p}p$

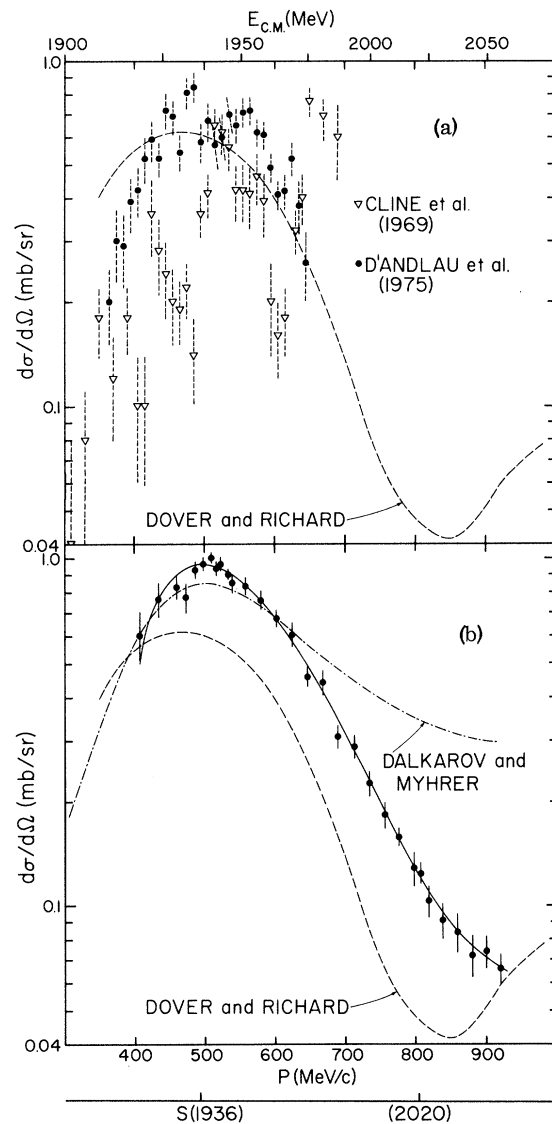


FIG. 3. (a) Previous measurement of $\bar{p}p \rightarrow \bar{p}p(\cos\theta_{c.m.} \leq -0.8)$. The curve is a potential model calculation of Dover and Richard (Ref. 21). (b) Results of this experiment. The solid curve is a fifth-order polynomial fit to our data. The dashed curve is the potential-model prediction of Dover and Richard (Ref. 21) and the dot-dash curve represents that of Dalkarov and Myhrer (Ref. 22).

scattering at 180° as a function of incident momentum is shown in Fig. 3(b), and is also tabulated in Table I. The errors shown are statistical only and average about 6% in the S region and 10% near $p_{\bar{p}} = 805$ MeV/c ($E_{c.m.} = 2020$ MeV). We estimate that the systematic errors are about 4%.

The data show a broad smooth enhancement indicating the passage of the second diffraction maximum through 180° as the momentum changes.²³

TABLE I. Differential cross section at 180° ($\langle \cos\theta \rangle = -0.994$) for $\bar{p}p$ elastic scattering as a function of \bar{p} momentum (p).

p (MeV/c)	$d\sigma(180^\circ)/d\Omega$ (mb/sr)	p (MeV/c)	$d\sigma(180^\circ)/d\Omega$ (mb/sr)
406	0.602 ± 0.099	647	0.458 ± 0.031
434	0.765 ± 0.090	669	0.441 ± 0.038
460	0.825 ± 0.065	690	0.308 ± 0.024
473	0.776 ± 0.081	713	0.288 ± 0.022
486	0.928 ± 0.056	735	0.266 ± 0.019
498	0.964 ± 0.047	756	0.183 ± 0.016
510	1.011 ± 0.037	777	0.158 ± 0.010
516	0.937 ± 0.050	798	0.128 ± 0.015
523	0.965 ± 0.046	808	0.124 ± 0.008
534	0.905 ± 0.034	819	0.103 ± 0.011
540	0.851 ± 0.056	839	0.091 ± 0.011
558	0.833 ± 0.051	860	0.084 ± 0.011
581	0.760 ± 0.053	881	0.072 ± 0.010
603	0.673 ± 0.040	901	0.074 ± 0.008
625	0.607 ± 0.049	922	0.066 ± 0.007

The dashed curves are potential-model predictions^{21,22} neither of which agree well with our data. The solid curve is the result of a fifth-order polynomial fit to our data with a $\chi^2/\text{degrees of freedom}$ of 0.711. There is no evidence in this reaction, at the 0.1-mb/sr level, for a narrow resonance ($\Gamma < 10$ MeV) in the region of the S. In this region of 10-MeV/c spacing of the data points and the experimental momentum resolution (± 12 MeV/c) are approximately equal and correspond to ± 3 -MeV c.m. energy. In addition, we see no resonance near 805 MeV/c where $E_{\text{c.m.}} = 2020$ MeV. In both regions substantial structure is expected in the elastic channel associated with these resonances, both of which have been reported to be strongly coupled to the $\bar{p}p$ channel.²⁻⁶

We are grateful to the Brookhaven alternating-gradient synchrotron staff for their generous assistance and hospitality. We thank C. Wiegand for an emergency shipment of Rinso White for the water Cherenkov counter. We also thank T. Daly and M. Long for technical assistance throughout the experiment. This work was sup-

ported by the High Energy Physics Division of the U. S. Department of Energy under Contracts No. W-7405-ENG-48, No. ER-78-S-02-4831, and No. EY-76-C-02-0016. One of us (H.N.) would like to thank the Faculty Grants Committee of Mount Holyoke College and the University of Massachusetts Computer Center for financial support.

¹G. Chikovani *et al.*, Phys. Lett. **22**, 233 (1966); M. N. Focacci *et al.*, Phys. Rev. Lett. **17**, 890 (1966).

²P. Benkheiri *et al.*, Phys. Lett. **68B**, 483 (1977).

³A. S. Carroll *et al.*, Phys. Rev. Lett. **32**, 247 (1974).

⁴V. Chaloupka *et al.*, Phys. Lett. **61B**, 487 (1976).

⁵S. Sakamoto *et al.*, reported by S. Ozaki, in *Proceedings of the Nineteenth International Conference on High Energy Physics, Tokyo, 1978*, edited by S. Homma, M. Kawaguchi, and H. Miyazawa (International Academic Printing, Japan, 1979), p. 101.

⁶W. Brückner *et al.*, Phys. Lett. **67B**, 222 (1977).

⁷T. E. Kalogeropoulos and G. S. Tzanakos, Phys. Rev. Lett. **34**, 1047 (1975).

⁸G. Flugge, Rapporteur Talk, in *Proceedings of the Nineteenth International Conference, Tokyo, 1978*, edited by S. Homma, M. Kawaguchi, and H. Miyazawa (International Academic Printing, Japan, 1979), p. 793.

⁹Y. M. Antipov *et al.*, Phys. Lett. **40B**, 147 (1972).

¹⁰D. Bowen *et al.*, Phys. Rev. Lett. **30**, 332 (1973).

¹¹P. Benkheiri *et al.*, Phys. Lett. **81B**, 380 (1979).

¹²R. M. Bionta *et al.*, Bull. Am. Phys. Soc. **24**, 673 (1979).

¹³A. S. Carroll *et al.*, Bull. Am. Phys. Soc. **24**, 674 (1979).

¹⁴M. Alston-Garnjost *et al.*, Phys. Rev. Lett. **35**, 1685 (1975).

¹⁵R. Bizzarri *et al.*, Phys. D **6**, 160 (1972).

¹⁶J. Lys, Phys. Rev. **186**, 1691 (1969).

¹⁷D. Cline *et al.*, Phys. Rev. Lett. **21**, 1268 (1968).

¹⁸Ch. D'Andlauer *et al.*, Phys. Lett. **58B**, 223 (1975).

¹⁹M. Alston-Garnjost *et al.*, Phys. Rev. D (to be published).

²⁰E. Bracci *et al.*, CERN/HERA Report No. 73-1, 1973 (unpublished).

²¹C. B. Dover and J. M. Richard, private communication.

²²O. D. Dalkarov and F. Myhrer, Nuovo Cimento **40A**, 152 (1977).

²³E. Eisenhandler *et al.*, Nucl. Phys. **B113**, 1 (1976).